LANGMUIR

pubs.acs.org/Langmuir Article

Differential Interactions of Piscidins with Phospholipids and Lipopolysaccharides at Membrane Interfaces

Hannah Cetuk, Joseph Maramba, Madolyn Britt, Alison J. Scott, Robert K. Ernst, Mihaela Mihailescu, Myriam L. Cotten, and Sergei Sukharev*



Cite This: Langmuir 2020, 36, 5065-5077

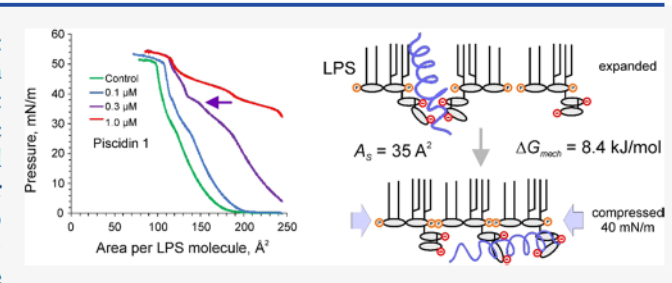


ACCESS

III Metrics & More

Article Recommendations

ABSTRACT: Piscidins 1 and 3 (P1 and P3) are potent antimicrobial peptides isolated from striped bass. Their mechanism of action involves formation of amphipathic α -helices on contact with phospholipids and destabilization of the microbial cytoplasmic membrane. The peptides are active against both Gram-positive and Gram-negative bacteria, suggesting easy passage across the outer membrane. Here, we performed a comparative study of these two piscidins at the air—water interface on lipopolysaccharide (LPS) monolayers modeling the outer bacterial surface of Gram-negative



organisms and on phospholipid monolayers, which mimic the inner membrane. The results show that P1 and P3 are highly surface active ($\log K_{\rm AW} \sim 6.8$) and have similar affinities to phospholipid monolayers ($\log K_{\rm lip} \approx 7.7$). P1, which is more potent against Gram negatives, exhibits a much stronger partitioning into LPS monolayers ($\log K_{\rm LPS} = 8.3$). Pressure—area isotherms indicate that under increasing lateral pressures, inserted P1 repartitions from phospholipid monolayers back to the subphase or to a more shallow position with in-plane areas of $\sim 170~{\rm \AA}^2$ per peptide, corresponding to fully folded amphipathic α -helices. In contrast, peptide expulsion from LPS occurs with areas of $\sim 35~{\rm \AA}^2$, suggesting that the peptides may not form the similarly oriented, rigid secondary structures when they avidly intercalate between LPS molecules. Patch-clamp experiments on *Escherichia coli* spheroplasts show that when P1 and P3 reach the outer surface of the bacterial cytoplasmic membrane, they produce fluctuating conductive structures at voltages above 80 mV. The data suggests that the strong activity of these piscidins against Gram-negative bacteria begins with the preferential accumulation of peptides in the outer LPS layer followed by penetration into the periplasm, where they form stable amphipathic α -helices upon contact with phospholipids and attack the energized inner membrane.

■ INTRODUCTION

Antimicrobial peptides (AMPs) identified in a number of vertebrates are promising therapeutic agents. ^{1,2} These peptides, typically 20–50 residues in length, are effective against a broad spectrum of bacteria while producing a low incidence of induced bacterial resistance due to their primarily membrane-focused interactions with their targets. ^{1–3} Some peptides have anesthetic ⁴ and even immunomodulatory effects, ⁵ revealing their ability to act not only on bacterial membranes but also on mammalian host cell receptors.

Piscidins are AMPs found in teleost fish where they are key components of innate immunity.⁶ The isoforms P1 and P3, which are 22-amino-acid long and 68% homologous, were first isolated from the mast cells of hybrid striped bass.^{7,8} These peptides have proven potent against both Gram-positive and Gram-negative bacteria.^{9,10} Additionally, P1, which is active against viruses such as human immunodeficiency virus (HIV)-1¹¹ and pseudorabies,¹² induces apoptosis in cancer cells.¹³ However, the optimization of piscidins as drugs may require stabilization against protease degradation and an increase in selectivity by minimizing the often accompanying hemolytic

activity.¹⁴ A better understanding of the basic physicochemical mechanisms of piscidins may also allow for the design of agents with improved potency and selectivity based on their structural scaffold and unique principles of action.

It is commonly accepted that the main antibacterial effect of P1 is based on their ability to permeate the outer membrane and bind directly to the cytoplasmic bacterial membrane and disrupt its integrity. Sine earlier studies, piscidins have demonstrated the ability to change their conformation from an unstructured free form in solution to an amphipathic α -helix on contact with the phosphate-containing groups of detergents or phospholipids. The orientations of the partially submerged amphipathic piscidin helix, which can be either almost parallel to the bilayer plane or tilted, have been determined

Received: January 5, 2020 Revised: April 18, 2020 Published: April 20, 2020





using oriented-sample solid-state NMR, ^{9,16} neutron diffraction ¹⁷ and analyzed in extensive all-atom molecular dynamics (MD) simulations. ^{18,19} Our recent study comparing P1 and P3 has suggested that differing tilts, helical orientations, positions of histidines, amphipathicity, flexibility, and depths of insertion into the membrane are the factors that make P1 a stronger membrane-perturbing agent than P3. ^{17,20} In contrast, P3 was found to be more damaging to DNA. ²¹

On a molecular level, it has been proposed that AMPs form flexible toroidal pores with a peptide-stabilized rim that likely results from thinning of the bilayer and curvature generation by the peptide. 16,18 One of the questions that remains poorly understood is how these peptides discriminate their action between vertebrate and bacterial cell membranes. Most bacteria maintain a high electrical potential gradient on their cytoplasmic membrane relative to eukaryotes and also have membranes containing a high mole fraction of negatively charged lipids.²² Like many cationic AMPs, P1 and P3 would likely have a greater affinity to these negatively charged bacterial membranes than to eukaryotic host cells. 23,24 Another hypothesis is that the presence of cholesterol in the phosphatidylcholine (PC)-dominated outer leaflet of the mammalian membrane somehow prevents piscidin insertion. This problem was partially addressed in our previous paper²⁰ where the analysis showed that P1 and P3 can produce demixing in phosphatidylcholine (PC)/cholesterol membranes. In bilayers containing phosphatidylethanolamine (PE), a lipid highly abundant in bacterial cell membranes, they increase the temperature at which the lamellar-tohexagonal phase transition appears. Contrary to expectation, these recent studies show that the presence of cholesterol in membranes does not reduce the permeabilizing capacity of P1 and the question of specificity and preference toward the bacterial cell envelope remains open.

The outer membrane of Gram-negative microorganisms, composed of lipopolysaccharides (LPS) and phospholipids, is a formidable barrier for many antimicrobial agents. For this reason, many drugs exhibit considerably higher minimum inhibitory concentrations (MICs) for Gram-negative microorganisms than for Gram positives. Yet, the MICs of P1 toward Gram-positive and Gram-negative bacteria are comparable (2–4 μ M for *Staphylococcus aureus* and 2–10 μ M for *Escherichia coli*, respectively $^{8-10,21}$). This potency against Gram negatives poses another puzzle and calls for detailed studies of piscidin interactions with LPS, the main component of the external leaflet of the Gram-negative bacterial outer membrane.

We address this problem here by studying the interfacial properties of piscidins and examining their affinities to both phospholipid and LPS monolayers using the Langmuir technique. 27,28 Incorporation of piscidins from the subphase into the monolayer increases the area at a given pressure relative to controls with no piscidin. The analysis of isotherms allows for estimations of partitioning coefficients and the molecular area parameter, which influence the partitioning equilibria. 27,29-31 The data presented shows a considerably higher affinity and more shallow pressure dependence of partitioning in LPS compared to phospholipids, signifying a different character of piscidin interactions with these two different chemical environments. This suggests that the peptides, especially P1, massively accumulate in the outer LPS layer where they may permeate through the leaflet as partially unstructured chains.

We also approach interactions of piscidins with the native cytoplasmic membrane of E. coli using the patch-clamp technique applied directly to giant bacterial spheroplasts. We show that when applied from either the periplasmic (or cytoplasmic) side, P1 and P3 produce conductive structures in the native bacterial membrane activated at moderate hyper- or depolarizing voltages, which is a result previously observed only in model lipid membranes. 15 Patch-clamp recordings also show that the peptides presented to the periplasmic side of the inner membrane predispose mechanosensitive (MS) channels MscS and MscL to opening by a slightly lower tension; however, comparison of growth curves of wild type (WT) and $\Delta mscL$, $\Delta mscS$, and $\Delta mscK$ E. coli strains indicates that activation of mechanosensitive channels may not be the key component of the growth suppression mechanism by the piscidins.

■ EXPERIMENTAL SECTION

Materials. The piscidin 1 (P1 FFHHIFRGIVHVGKTIHRLVTG-NH2) and piscidin 3 (P3 FIHHIFRGIVHAGRSIGRFLTG-NH2) peptides were synthesized using Fmoc-chemistry at the University of Texas Southwestern Medical Center (Dallas, TX). Next, they were purified by reverse-phase high-performance liquid chromatography (HPLC) on a C18 column using aceteonitrile/water with 0.1% trifluoroacetic acid as the mobile phase and characterized by mass spectrometry at William and Mary using a previously published protocol. 9,32 Washes with dilute HCl, dialysis, and multiple cycles of lyophilization/dissolution in nanopure water were performed to substitute chloride for trifluoroacetate ions. The final solution was analyzed by amino acid analysis (AAA) at the Protein Chemistry Lab at Texas A&M University (College Station, TX), thereby confirming the amino acid content and characterizing the peptide concentration.

The lipid mixture mimicking the inner membrane of *E. coli* for monolayer experiments was composed of 1-palmitoyl-2-oleoyl-sn-glycero-3-phosphoethanolamine (POPE), 1-palmitoyl-2-oleoyl-sn-glycero-3-phospho-glycerol (POPG), and cardiolipin (CL) purchased from Avanti Polar Lipids (Alabaster, AL).

Lipopolysaccharide (LPS-Re) was extracted from the D31m4 deep rough (Re) mutant strain of E. coli³³ using the phenol-chloroformpetroleum ether (PCP) method³⁴ with the following modifications. The bacterial pellet from 1 L of the overnight culture was washed sequentially (3500g for 10 min at room temperature) with 50 mL volumes of water (twice), 90% ethanol (thrice), acetone (thrice), and diethyl ether (twice) and dried under a nitrogen atmosphere. Dry, washed pellets were finely ground into powder and extracted in 20 mL of 2:5:8 (v/v/v) solution of 90% phenol/chloroform/petroleum ether for 30 min at 10 °C with vigorous stirring. The extraction solution was cleared by centrifugation at 5000g for 10 min at 4 °C and collected by aspiration. The extraction of this pellet was repeated once in fresh solution and both cleared supernatants were combined, dried under a stream of nitrogen, and residual chloroform/petroleum ether was removed by vacuum. Following water precipitation of LPS as described, 34' the pellet was washed five times in 50 mL volumes of 5:1 (v/v) diethyl ether/acetone and three times with 90% ethanol (3500g for 10 min at room temperature). The resulting pellet was dried, resuspended in water, briefly sonicated to disaggregate, and lyophilized. The polysaccharide chain in this Re mutant is short and truncated at the second 2-keto-3-deoxyoctonate (KDO) moiety and the polar part carries two phosphate and two carboxylate groups.

E. coli strains used in patch-clamp and growth rate experiments were Frag1 (wild type) and isogenic triple deletion mutant MJF465 ($\Delta mscL$, $\Delta mscS$, $\Delta mscK$) derived from Frag1.³⁵ The strains were gifts from Dr. Ian Booth (University of Aberdeen, U.K.).

Tensiometry. Surface tensions were measured at the air—liquid interface with varying concentrations of P1 and P3 in the subphase. Tensiometry was carried out in the buffer common for all surface tension and phospholipid monolayer experiments, which contained 200 mM KCl, 5 mM CaCl₂, 10 mM MgCl₂, and 5 mM N-(2-

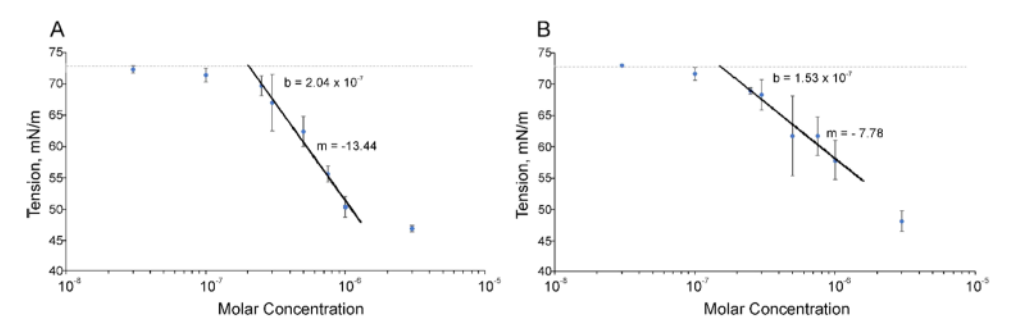


Figure 1. Gibbs isotherms for P1 (A) and P3 (B) in HEPES buffer. The intercept with the horizontal line at 72.8 mN/m signifies the air—water partition coefficient (K_{AW}), whereas the slope reflects the molecular area at the interface. Each point represents the average surface tension and error bars represent standard deviations (n = 4). The estimated K_{AW} and molecular areas are presented in Table 1.

hydroxyethyl)piperazine-N'-ethanesulfonic acid (HEPES) adjusted to pH 7.4 with KOH. The Kibron MicroTrough XS sensor equipped with a DyneProbe metal alloy needle as a Wilhelmy plate was zeroed to 0 mN/m in air prior to submersion in the buffer. The subphase with increasing concentrations of piscidin was loaded on a Teflon multiwell plate (Kibron Inc.). The subphase wells were allowed to equilibrate with specific concentrations of piscidins for approximately 40 min before surface tension measurements were taken. Surface tension measurements were carried out by steadily raising and lowering the probe into and out of the solution, with the maximum pressure over one of these cycles taken as the surface tension. One trial of surface tension measurements was determined by averaging the maximum tensions of 10 consecutive pulling cycles. A minimum of four trials was done at each piscidin concentration to obtain independent surface tension measurements that could be averaged and used for calculations. Treatment of Gibbs isotherms was based on the previous analysis. 30,36,37 Tensions obtained at different peptide concentrations were fitted with the Gibbs isotherm, $d\Upsilon/(d \ln C) =$ $-RT\Gamma$, to obtain the molecular area (A_S) , where Υ is the surface tension, C is the concentration of the amphipathic substance in solution, R is the gas constant, and T is the absolute temperature. Γ is equal to $(N_A A_S)^{-1}$, where N_A is Avogadro's constant. The air-water partition coefficient (KAW) was determined as the intercept of the Gibbs isotherm fit to the surface tension of buffer only (72.8 mN/m).

Langmuir Experiments and Analysis of Isotherms. Langmuir isotherms were taken using a two-barrier rectangular 22 cm × 6 cm MicroTrough XS equipped with a MicroSpot surface potential meter (Kibron Inc., Helsinki, Finland). Experiments were done in an airclean hood to minimize contamination. Potentiometric data was measured using the MicroSpot surface potentiometer (Kibron, Inc.) and pressure data was obtained using the Dyneprobe alloy probe. The phospholipid mixture used consisted of 86% POPE, 10% POPG, and 4% CL from Avanti Polar Lipids (Alabaster, AL) dissolved in chloroform to a final concentration of 0.2 mg/mL. The subphase buffer for phospholipid experiments is listed above. Following placement of the probe in the subphase, the tension and potential sensors were zeroed to 72.8 mN/m and 0 mV, respectively, before each trial. The lipids were deposited onto the subphase using a 50 μ L Hamilton syringe (Hamilton, Reno, NV). Isotherms were performed at 20 ± 1 °C at a barrier rate of 20 mm/min, following a start delay of 10 min to allow for chloroform evaporation.

LPS was dissolved in chloroform using cycles of mild heating and sonication to a final concentration of 1.6 mg/mL. The subphase buffer for LPS monolayer experiments consisted of 3 mM Tris, 100 mM KCl, and 0.1 mM CaCl₂, pH balanced to 7.2 with HCl. Isotherms were taken using the same protocol as above. For both P1 and P3, two full sets of isotherms were done, with isotherms for each concentration measured at least three times each. Due to the possibility of peptide adsorption on hydrophobic surfaces, the subphase was aspirated but the trough was not washed between the repeats.

The analysis of compression isotherms in the presence of piscidins was performed, as described in ref 31. Briefly, the Langmuir data was

replotted as the natural log of the area taken by guest molecules versus surface pressure (Π). The region near the equivalence pressure (35-40~mN/m) was fit to a linear function, where the slope of the fit was used to calculate the average molecule area ($a_{\rm d}$) based on the equation $-kT~\text{d} \ln(\Delta A)/\text{d}\Pi = a_{\rm d}$, where T is the absolute temperature and k is Boltzmann's constant. The partition coefficient of the bulk monolayer interface ($K_{\rm lip}$) was calculated as the ratio of the mole fraction of the peptide in the monolayer to the mole fraction of the peptide in the bulk, 27,31 near the equivalence pressure (35~mN/m).

Preparation of Giant Spheroplasts and Patch-Clamp Experiments. Spheroplasts were generated from the E. coli strain Frag1.35 This strain natively expresses several mechanosensitive channels,³⁸ with MscS and MscL channels as dominant species. Standard steps of filamentous growth in the presence of cephalexin followed by cell wall digestion with lysozyme in the presence of ethylenediaminetetraacetic acid (EDTA) were described previously. 39,40 Patch pipettes of \sim 1.5 μ m inner diameter were pulled from borosilicate glass capillaries (Drummond Scientific #2-000-100). Measurements were done in inside-out excised patches. The spheroplast recording buffer contained (in mM): 200 KCl, 10 CaCl₂, 90 MgCl₂, and 5 HEPES (pH 7.2). Preprogrammed pressure stimuli (pulses, steps, and ramps) were delivered from the modified HSPC-1 pressure-clamp apparatus (ALA Instruments, Farmingdale, NY). Currents were measured at pipette voltages between -100 and +100 mV. The analysis of activation midpoint pressure shifts was done using PClamp-10 software.

Growth Rate Determination. Growth kinetics for WT Frag1 and MJF465 E. coli strains were compared. From standard overnight cultures, cells were diluted 1:100 into standard Luria-Bertani (LB) media and grown to optical density $(OD)_{600} = 0.1$. Cell cultures were then aliquoted into a 96-well microplate (Corning) at 200 μ L/well. The peptides were prepared via serial dilution and 10 μ L of each was added into the culture-containing wells to final concentrations ranging from 0.5 to 8 μ M for P1 and 8 to 24 μ M for P3. Wells without the added peptide were used as a growth control, and wells containing no cells were included as blanks. The cultures were placed on a shaker platform at 225 rpm and incubated at 37 °C. The OD₆₀₀ was recorded using a plate reader SpectraMax 5 (Molecular Devices) every 30 min for approximately 5 h until the stationary phase was reached. Growth for each peptide concentration and strain-type combination was recorded for four replicates on the same plate. The replicates were analyzed to obtain averages and standard deviations. The averages were used to generate growth curves. These growth curves were fitted using the following modified Gompertz equation

$$\log\left(\frac{N}{N_0}\right) = \log\left(\frac{\text{OD}}{\text{OD}_{\min}}\right) = A \exp(-\exp[\mu_{\max}(\lambda - t) + 1])$$
(1)

where $\frac{N}{N_0}$ and $\frac{\mathrm{OD}_t}{\mathrm{OD}_{\min}}$ are representative of the relative population size at time t, A is the upper asymptote corresponding to the stationary phase, μ_{\max} is the maximum growth rate defined as the tangent of the inflection point, and λ is the lag time defined as the x-axis intercept of this tangent. The generation time (T) was determined from 41

Table 1. Area Parameters and Partition Coefficients Extracted from Gibbs Isotherms at the Air—Water Interface and from Langmuir Pressure—Area Isotherms Obtained on Phospholipid Monolayers Formed from a Mixture Mimicking the Inner Membrane of Gram-Negative Enteric Bacteria and on LPS Monolayers^a

system	compound	region (mN/m)	slope (m/N)	$A_{\rm S}$ (Å ²)	$\log(K_{\mathrm{AW}})$	$log(K_{lip})@5 \text{ mN/m}$	log(K _{lip})@35 mN/m	log(K _{lip})@45 mN/m	n
A/W interface	P1			30 ± 1	6.69				
	P3			60 ± 1	6.81				
phospholipids	P1, 0.1 μM	39-41	413 ± 7	170 ± 5		8.05 ± 0.08	7.67 ± 0.10	7.08 ± 0.28	3
	P3, 0.1 μM	38-41	240 ± 34	97 ± 14		7.87 ± 0.09	7.74 ± 0.06	6.91 ± 0.11	4
LPS	P1, 0.1 μM	37-39	85 ± 27	35 ± 11		8.32 ± 0.05	8.26 ± 0.03	8.09 ± 0.03	4
	P3, 0.1 μM	37-39	176 ± 30	71 ± 12		7.55 ± 0.04	7.77 ± 0.03	7.60 ± 0.20	5

 $^{a}K_{AW}$ represents the partition constant at the bare air—water interface estimated from the intercepts of Gibbs isotherms (Figure 1). The area parameter (A_{S}) was obtained from the slope of compacting transitions between 37 and 41 mN/m (Figures 3 and 5). K_{lip} was calculated using mole fractions obtained from monolayer compression isotherms (Figures 2–5) at surface pressures of 5, 35, and 45 mN/m.

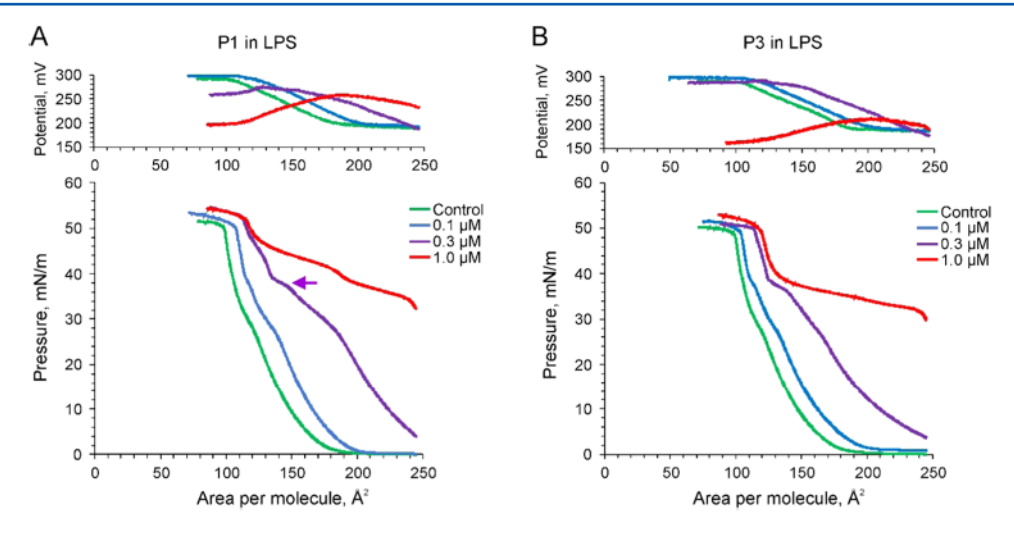


Figure 2. Pressure—area isotherms and surface potentials of LPS monolayers in the presence of P1 (A) and P3 (B) in the subphase. The presence of a pronounced shoulder on isotherms (especially at 0.3 μ M of peptides, arrow) signifies compaction or expulsion of peptides from the interface just below 40 mN/m, which correlates with flattening or decrease of the surface potential. Note that a fraction of the peptide stays intercalated at any pressure all of the way to collapse at about 50 mN/m and 120 Å² per molecule. LPS isotherms were obtained using a subphase Tris buffer (3 mM, pH 7.2) containing 100 mM KCl and 0.1 mM CaCl₂ at pH 7.2.

$$T = \frac{\log_{10}(2)}{\mu_{\text{max}}} \tag{2}$$

The fold increase was calculated as the ratio of generation times of the cultures with the peptide relative to controls and was used to evaluate the effect of the peptides on growth. When measurements were taken over the course of multiple days, the average fold increase between these days was calculated. The goodness of fit for the equations was determined using normalized root mean square error. All reported curves had a fit quality of 0.8 or higher.

RESULTS

Following previous studies, ^{30,42} we started with classical measurements of surface tension changes induced by P1 and P3 at the air—water interface. The tendency of a molecule to partition to the bare interface has been attributed primarily to the hydrophobic expulsion of the substance of interest from the bulk of aqueous solution. ^{30,43} Gibbs isotherms thus indicate the contribution of the pure hydrophobic effect to the total force driving the substance into the membrane and provide estimates of the molecular area at the air—water interface. The difference of the partitioning coefficients calculated from surface activity at the bare water interface and from the lipid monolayer compression isotherms will, in turn, indicate the contribution of specific interactions with the

lipids and the effect of varied lateral pressure on the partitioning of a molecule.

Surface Activity of Piscidins. Figure 1 presents Gibbs isotherms for P1 and P3 measured in the KCl-HEPES buffer with Mg^{2+} to standardize the electrolyte conditions for binding. The intercepts indicate very comparable air—water partitioning coefficients (K_{AW}) , 30 but different slopes indicate different areas (Table 1) and possibly suggest that the peptides interact with the interface using differing conformations. P1 interacts with a smaller effective area, thus forming a more compact or differently oriented particle. In the assumption that the two peptides have similar conformations in aqueous solutions, the about 2-fold difference between the molecular areas may also suggest dimerization of P3.

Langmuir Experiments. Figure 2 shows pressure—area isotherms and concomitantly measured surface potentials of LPS monolayers in the presence of P1 and P3. Given that piscidins evolved in cold-blooded organisms, the experiments were conducted at room temperature. The control curve of LPS on a pure subphase indicates a small shoulder, corresponding to facilitated compaction of LPS between 26 and 30 mN/m. The change in the area per lipid from 250 Å² in the expanded state to collapse at ~110 Å² results in a positive change of the surface potential by ~100 mV. We note that

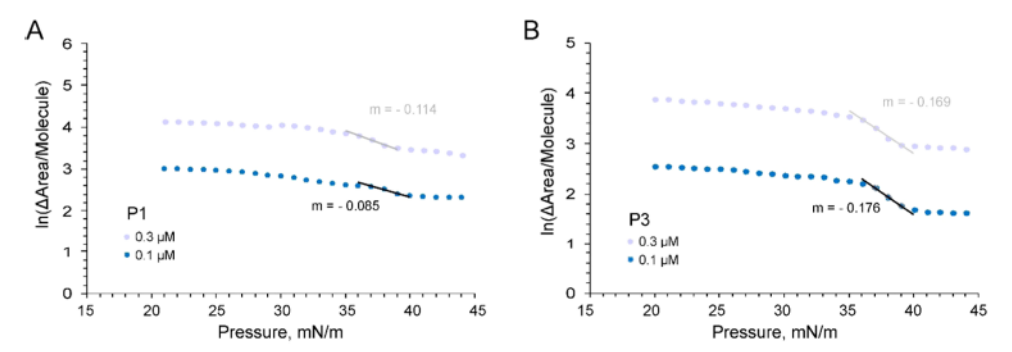


Figure 3. Semilogarithmic plots of differential monolayer areas plotted as functions of surface pressure of LPS for P1 (A) and P3 (B). The differential areas were calculated relative to peptide-free controls. The linear regions of these curves fitted with straight lines represent the shoulders signifying the process of peptide compaction or expulsion from the film. As explained in Experimental Section, the slope gives an estimate of molecular areas that the peptides occupy in the plane of the monolayer.

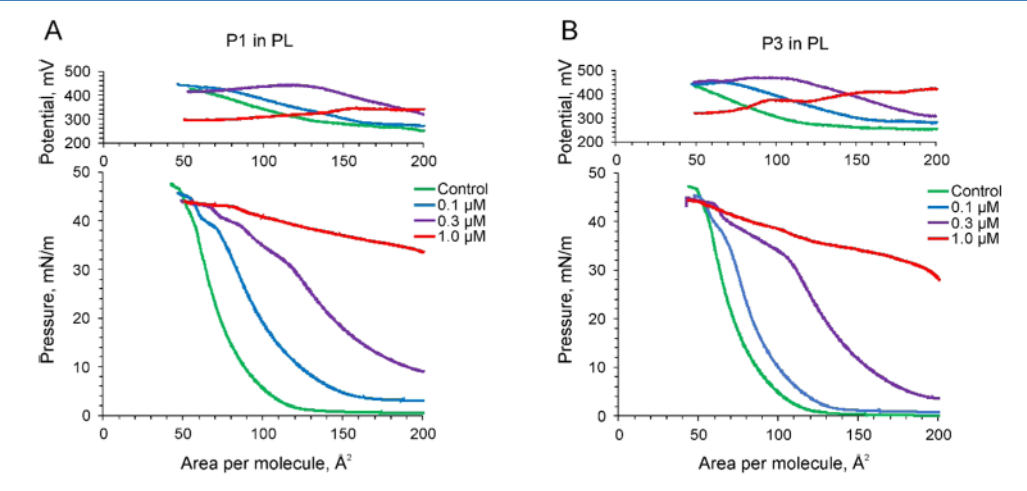


Figure 4. Pressure—area isotherms and surface potentials of phospholipid monolayers in the presence of P1 (A) and P3 (B) in the subphase. The presence of a pronounced shoulder on isotherms near 40 mN/m (at 0.1 μ M, blue curves) and above 32–33 mN/m (at 0.3 μ M of peptides, purple curves) signifies expulsion of peptides from the phospholipid layer, which also correlates with flattening or decrease of the surface potential. The phospholipid isotherms were obtained using a subphase HEPES buffer (5 mM, pH 7.4), containing 200 mM KCl, 10 mM MgCl₂, and 5 mM CaCl₂.

even in control experiments, the interfacial potential of negatively charged LPS monolayers is positive (+200-300 mV), indicating the presence of a strong positive dipole component, as in phospholipids. The effect of peptides is clearly visible already at 0.1 μ M, manifested as an almost parallel right shift of the isotherm, preserving the features of the control curve and a positive shift of the potential. At 0.3 μ M, we see a massive swelling of the monolayer in the expanded state and a more pronounced shoulder between 28 and 40 mN/m, signifying partial redistribution of the peptide from the film back to the subphase or to a shallower position, e.g., less inserted in the hydrocarbon. This transition reflects two contributions to the free energy of intercalation, the negative chemical ΔG_{chem} that drives the peptide into the lipid and the positive mechanical energy term, $\Delta G_{\text{mech}} = p \cdot A_{\text{S}}$, where As is the cross-sectional area of the "guest" molecule. Compression of the monolayer increases the lateral pressure p, which counteracts the insertion by adding a positive mechanical energy term. At 1.0 µM, both peptides drastically distort the isotherms due to massive partitioning into the expanded film and then expulsion with compression. Importantly, the surface potential curves reverse their course at higher peptide concentrations (especially for P1) apparently due to the expulsion of the positively charged peptides from the film and possible changes in the film structure.

In the previous studies, the swelling of monolayers by membrane-active drugs was used to estimate their partition coefficients.²⁷ In this study, we extend this type of analysis by monitoring the equilibrium partitioning of the peptides as a function of surface pressure. The amount of the guest molecule residing among the lipids is measured as the monolayer area relative to the control peptide-free isotherm. The most characteristic segments of isotherms are the "shoulders" where the logarithmic slope of the differential area change with pressure reflects the effective area with which the guest molecule redistributes between the core of the monolayer and a more shallow position or the subphase.³¹ Figure 3 shows the data from Figure 2 replotted as the log of differential area versus surface pressure for 0.1 and 0.3 µM concentrations of P1 and P3 peptides. The estimated molecular areas for P1 and P3 as they are expelled from the LPS monolayer (see Figure 3 and Experimental Section) are ~35 and 71 Å², respectively. Taking into account these areas, we estimate the water-LPS (K_{lip}) partition coefficients (at 35 mN/m) as ~1.8 × 10⁸ for P1 and 5.9×10^7 for P3 presented as $\log(K_{\text{lip}})$ of 8.26 and 7.77 in Table 1. P1 has a markedly higher affinity for the LPS monolayer.

We performed similar experiments with phospholipid monolayers, mimicking the composition of the inner membrane of typical Gram-negative bacteria.²² As shown in

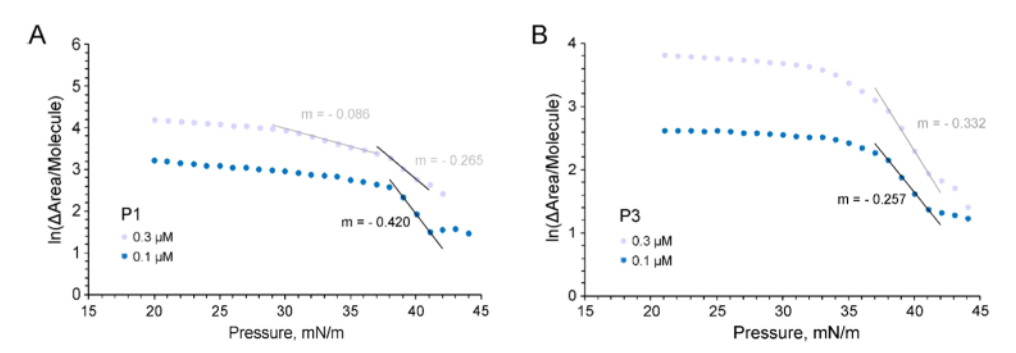


Figure 5. Semilogarithmic plots of differential phospholipid monolayer areas relative to peptide-free controls plotted as functions of surface pressure for P1 (A) and P3 (B). The inclined regions of these curves fitted with straight lines signify the process of peptide compaction or expulsion from the film. As explained in Experimental Section, the slope provides an estimate of the molecular area that the peptides take in the plane of the phospholipid monolayer. As seen from (A), P1 present at a higher concentration $(0.3 \, \mu\text{M})$ experiences a shallow pretransition (fitted with a gray line), which may represent a reorientation or compaction. These areas are 3–5 times larger than the areas estimated from the LPS monolayers (Figure 3 and Table 1).

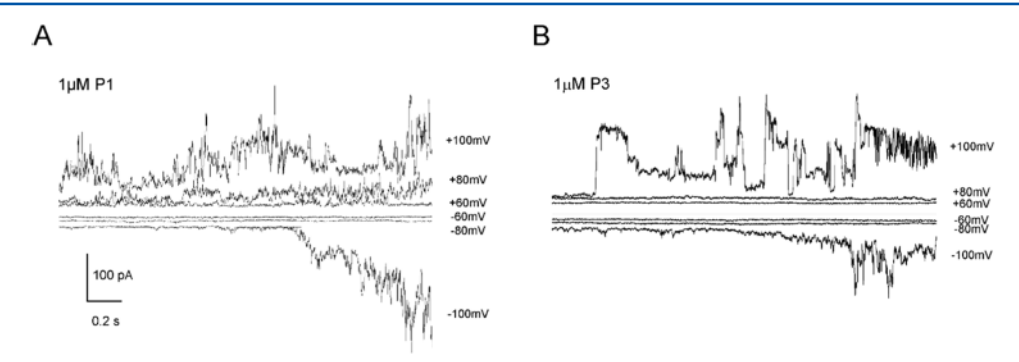


Figure 6. Pore-forming capacity of piscidins in the inner membrane of *E. coli*. Current fluctuations in the *E. coli* inner membrane were recorded at different voltages in excised patches in the presence of $1.0~\mu M$ P1 (A) and $1.0~\mu M$ P3 (B). Piscidins were added to the periplasmic side of the membrane through the pipette. The numbers by traces represent voltages in the pipette relative to the bath.

Figure 4, P1 and P3 both show strong incorporation even at a concentration of 0.1 µM. At lateral pressures between 37 and 40 mN/m (i.e., near the monolayer-bilayer equivalence pressure^{28,46}), P1 present at 0.1 or 0.3 μ M in the subphase exhibits a characteristic shoulder, which is absent in the controls. At 0.3 µM, P1 exhibits another pretransition with the onset near 32 mN/m. The P3 isotherms display one transition starting at 35-37 mN/m, and at 40-42 mN/m we observe a closer convergence with the control, signifying a nearly complete expulsion from the lipid. In controls and at low peptide concentrations, surface potential grows with compression, covering the range of ~250 mV. Note that at high concentrations, the interfacial potential behaves nonmonotonously (Figure 4A,B), reflecting massive expulsion of positively charged peptides from the surface layer and likely disruption of the monolayer structure.

The analysis of slopes at the isotherm shoulders presented in Figure 5 shows that the main peptide expulsion from a phospholipid monolayer occurs with a considerably higher slope compared to LPS. The slope for P1 corresponds to \sim 170 Ų (Table 1), which is equal to the footprint of about three to four lipid molecules at this pressure. This suggests that the peptides interact with the phospholipids differently than either the LPS monolayer or the bare air—water interface and likely form rigid α -helices oriented parallel to the interface, as previously illustrated by NMR studies 16 and MD simulations. 18

The summary of peptide affinities to different interfaces and associated molecular areas is presented in Table 1. A strong propensity to the air—water interface indicates a considerable

contribution of hydrophobic effect in the total surface activity. The presence of phospholipids and especially LPS further increases the affinity toward the interface, by 1 and 2 orders of magnitude, respectively. P1 exhibits a considerably larger inplane area when adsorbed on phospholipid monolayers, but a much smaller area and higher partition coefficient toward LPS monolayers, which indicates a different type of interaction with each molecular environment. We present the expulsion areas $(A_{\rm S})$ measured at the lowest concentration of the guest molecule $(0.1~\mu{\rm M})$ to avoid strong inhomogeneity due to the high guest molecule's mole fraction in the monolayer.

Comparing the free energies associated with the initial partitioning of peptides into the relaxed monolayer with the work of compaction and partial expulsion by ramped up pressure indicates a drastic difference between phospholipids and LPS. For phospholipids, the P1 $log(K_{lip})$ of 8.05 translates to a free energy of 46.2 kJ/mol and favors partitioning into a continuous expanded monolayer at p = 5 mN/m. At p = 38mN/m, half of the peptide, which covers 170 Å² in the plane of the monolayer, is expelled to a shallower position. This process is driven by the term $p \times A_S = 38.9 \text{ kJ/mol}$, which negates the majority of the binding energy. This indicates that unbinding from this shallow position back to the bulk would only take about 7.3 kJ/mol, i.e., shallowly bound peptide molecules have relatively low affinity to phospholipids. This illustrates, however, that P1 has sufficient affinity to insert itself into the phospholipid bilayer at lateral pressures of 35-38 mN/m near the monolayer-bilayer equivalence pressure, 46 but not far beyond that.

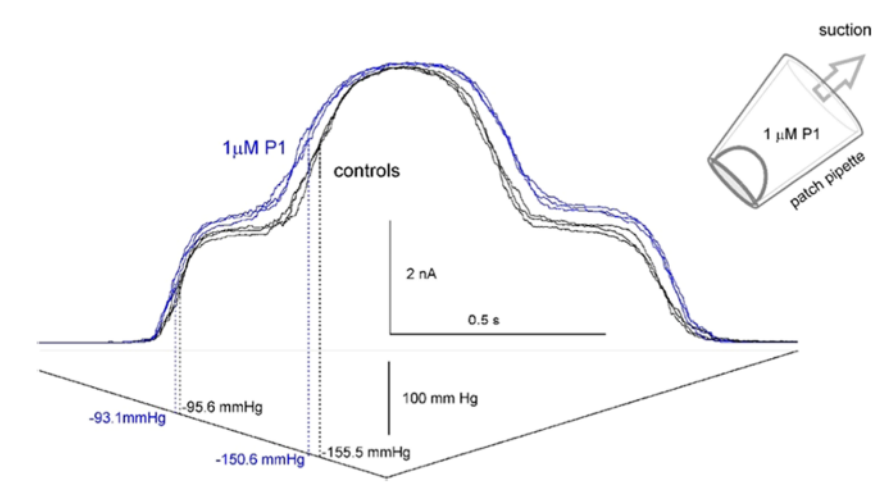


Figure 7. Effect of P1 on activation of MscS and MscL by tension. P1 was added to the pipette behind a sucrose "plug" in the tip. The family control curves were recorded at +30 mV (pipette voltage) with three repeated triangular pressure ramps as a stimulus immediately after gigaseal formation. The test curves were recorded on the same patch 30 min later, allowing for P1 diffusion through the plug to the membrane. All curves show two sequential waves of MscS and MscL activation. The effect of P1 is seen as a small leftward shift of both MscS and MscL activation midpoints.

The compacting transition in LPS in the presence of P1 takes place at the same surface pressure of ~ 36 mN/m, but with a 4 times lower area ($A_{\rm S}=35$ Ų). The initial insertion between LPS in the beginning of compression (5 mN/m) is driven by 47.8 kJ/mol of free energy, but the relatively small compacting transition starting at 36 mN/m takes only 8.4 kJ/mol, which (i) leaves a substantial fraction of P1 still inserted and (ii) shows that the energy difference between this "squeezed" P1 population and the unbound P1 in solution would be ~ 39.4 kJ/mol. Therefore, at high lateral pressures (>40 mN/m), all of the way to the film collapse, a large fraction of P1 remains tightly bound to the LPS layer. The illustration of this difference between phospholipid and LPS is given in the form of thermodynamic cycles (Figure 9).

Patch-Clamp Experiments on Bacterial Spheroplasts. Previously, antimicrobial efficacies of piscidins were studied in live bacterial cultures, 8,10,21,47 whereas membranotropic effects were recorded primarily in model membranes. 10,17,20,47-49 In addition, single-pore conductance measurements were performed in planar bilayer membranes. 15 The latter indicated high potency of piscidins in creating irregular conductive structures, especially at high voltages. Here, we present piscidin-induced currents recorded directly from the cytoplasmic membrane of E. coli. Giant spheroplasts were prepared from Frag1, a wild-type E. coli strain. Excised inside-out patches were subjected to piscidins from either the cytoplasmic side (bath) or periplasmic side (through the pipette). Figure 6 shows currents recorded with 1.0 µM piscidins. Consistent with the previous results, 15 an increase of voltage nonlinearly increases current, which fluctuates irregularly. In this specific configuration, the current increased more readily under positive pipette voltages (hyperpolarization, negative inside). These results are consistent with the hypothesis that, by destabilizing the membrane, piscidins decrease the critical voltage of electrical breakdown to below normal voltages of the energized bacterial membrane, which normally exceed 150 mV.50,51

Utilizing the Frag1 giant spheroplast preparations and patchclamp technique, we were able to record the effects of piscidins not only on the conductive properties of native bacterial membranes but also on mechanosensitive channels residing in the inner membrane. Previously, it was shown that intercalation of many amphipathic substances into the inner leaflet of the cytoplasmic membrane shifts activation curves to the right, requiring more tension for opening of mechanosensitive channels. This effect was interpreted as a result of increased lateral pressure, which requires stronger tension to overcome it. The exception was the amphipathic peptide GsMTx4, which left-shifted activation curves effectively, facilitating activation of MS channels. Piscidins, when presented from the cytoplasmic side, produced an effect similar to GsMTx4, shifting activation midpoints of MscS and MscL to the left by about 20%, thus assisting earlier activation. Description of the cytoplasmic side and the left by about 20%, thus assisting earlier activation.

The experiment presented in Figure 7 aimed at recording the effect of piscidins acting specifically on the outer (periplasmic) side of the inner membrane. The tip of the pipette was filled to about 4 mm with the pipette solution supplemented with 0.5 M sucrose to increase viscosity. The pipette was than backfilled with a regular pipette solution containing 1.0 μ M of P1. It is known that diffusion of small substances across the 4 mm sucrose-filled gap takes about 20 min. Thus, first recordings were made immediately upon the gigaseal formation with the spheroplast (which takes 5-10 min) and these were considered control traces. The traces recorded with a triangular pressure ramp show two waves produced by sequential activation of MscS and MscL channels. Subsequent recordings with the same triangular ramp stimuli were made after a 30 min waiting time, allowing for the diffusion of P1. The interaction of P1 with the outer surface produced a very small leftward shift of the activation midpoints.

Growth Rate Experiments with Bacterial Strains Devoid of MS Channels. To test whether or not piscidins may compromise the barrier function of the cytoplasmic membrane by targeting MS channels and predisposing them to activate, MICs of the WT $E.\ coli$ strain (Frag1) and isogenic strain devoid of three major mechanosensitive channels (MJF465 $\Delta mscL$, $\Delta mscS$, and $\Delta mscK$) were determined. Each culture was pregrown to OD of 0.1 in a flask and then aliquoted into a 96-well plate when piscidins were added over a range of different concentrations. The plate was kept in a

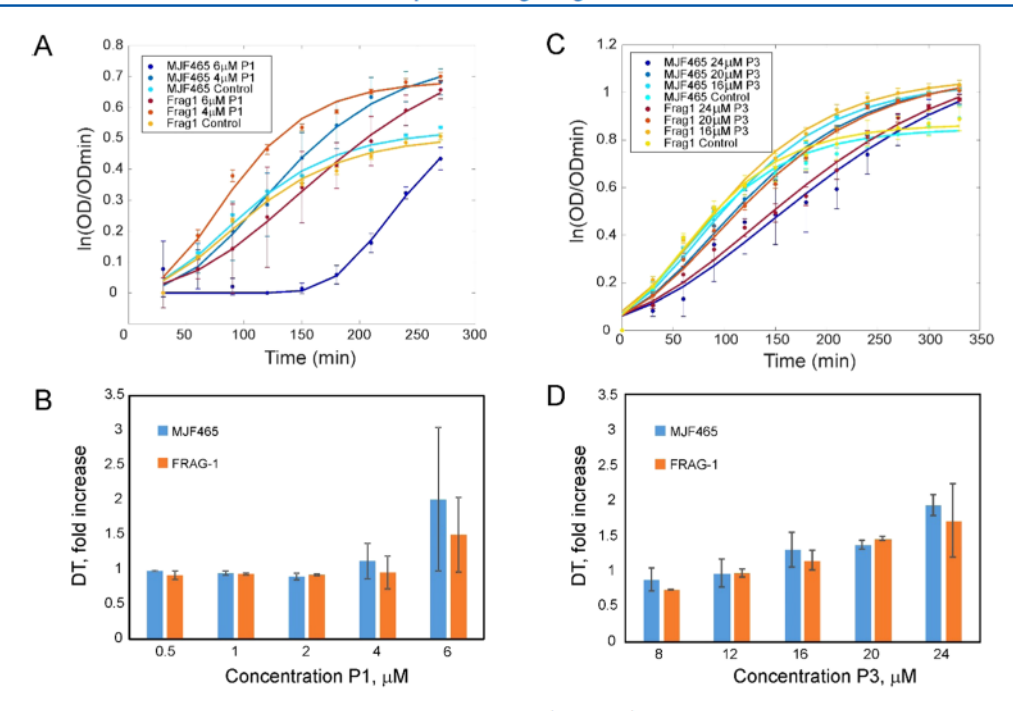


Figure 8. Growth parameters of the triple MS channel deletion E. coli strain (MJF465) in the presence of different concentrations of P1 and P3 in comparison with the WT strain (Frag1). Growth curves (A) fitted with the modified Gompertz equation (see Experimental Section) and the fold of duplication time (DT) increase (B) in the presence of P1. (C, D) Illustrate the same data for P3. Fitting of growth curves shows that the MJF465 strain experiences a stronger retardation with both peptides. The DT data show no statistical difference between the strains at any piscidin concentration. In the presence of P3, there was not a significant increase in DT between the lowest and highest concentrations for Frag1, whereas the increase in DT for MJF465 between these P3 concentrations was significant (p-value = 0.02). There was no statistical difference between the lowest and highest P1 values for either strain; however, by 8 μ M P1, both strains were killed off completely.

shaker and OD readings were taken every 30 min. We have noticed that adding antimicrobial peptides at the cell density of 0.1 was optimal for growth curve measurements. When the peptides were added together with a small cell inoculum, growth was delayed by approximately 3 h, but final growth curves ignoring the initial lag period were indistinguishable from controls, apparently due to peptide degradation in the culture.

Figure 8 depicts growth curves for Frag1 and MJF465 strains, all starting at $OD_{600} = 0.1$ in the presence of varied concentrations of P1 or P3. Panels A and C present the growth data in the semilog scale. The curves show that at P1 concentration up to 4.0 µM we do not see statistically significant growth inhibition. However, 6.0 µM becomes inhibitory and 8.0 µM stops growth completely. Panels B and D show the fold of duplication time (DT) change with P1 and P3 concentrations, respectively. Panel C indicates that even a slight inhibition of the growth rate requires about 3 times higher concentrations of P3. The growth stimulation effect at low peptide concentrations was also present with P3, though the fold of duplication time rose more gradually with P3 concentration. The cumulative data obtained in five independent experiments have shown that the wild-type strain is equally susceptible to piscidins as the triple deletion strain, as we found no statistically significant difference between the strains (Figure 8, caption). Therefore, MS channels present in WT do not appear to sensitize Frag1 to peptides in this experimental setting.

In this study, we used the traditional tensiometry and Langmuir techniques to obtain comparative data on P1 and P3 interactions with air—water, phospholipid, and LPS interfaces. This approach provides us with the very first "macroscopic"

survey of piscidin—LPS interactions and yields estimates of thermodynamic and molecular area parameters that will instruct future studies involving more precise structural techniques and simulations. The advantage of a lateral pressure-controlled monolayer system, representing half membranes, compared to full bilayer membrane model systems is that the interaction with the guest molecules can be measured at different areas per molecule. The varied density of monolayer packing provides the guest access to all parts of lipid molecules, not only to headgroups, potentially allowing one to probe equilibria at different depths of penetration and to separate the chemical component of insertion energy from the mechanical component.

Although temperature effects on phase behavior⁵³ and mechanical properties⁵⁴ of LPS have been reported before, we chose room temperature for our experiments because piscidins evolved in cold-blooded organisms and fulfill their protective role at low ambient temperatures. Compaction of LPS monolayers at room temperature, however, begins in the liquid-expanded state and, with gradual compression of the monolayer, proceeds to a condensed state at high lateral pressures all of the way to collapse above 50 mN/m. This process encompasses the range of states normally occupied by lamellar lipid phases at temperatures both above and below the lipid phase transition temperature. To illustrate the insertion of the peptides over the range of monolayer compaction states, we report partition coefficients for piscidins at 5, 35, and 45 mN/m. This data clearly shows that peptide insertion is opposed by compaction and can be similarly hindered by freezing

The Gibbs isotherms indicated that both P1 and P3 are highly surface active and likely form amphipathic structures

when at the air-water interface. The comparison of partition coefficients deduced from Gibbs and the pressure-area Langmuir isotherms indicates that initially the peptides are hydrophobically driven to the interface (log $K_{AW} \sim 6.7$), but in the presence of phospholipids held at low lateral pressure the partition coefficient $\log K_{lip}$ for P1 increases to 8.05. This translates into a purely hydrophobic component of -38.5 kJ/ mol, driving the peptide out of water (according to the Gibbs isotherm), and -46.2 kJ/mol, characterizing the phospholipid monolayer as a more favorable environment (by -7.7 kJ/mol) compared to the air-water boundary. The stronger attraction to LPS further increases the coefficient, indicated by a $log K_{lip}$ value of 8.3, which translates to a binding energy of 47.8 kJ/ mol. The decisive contribution of hydrophobic expulsion to the membrane binding energy for many amphipathic substances has been emphasized previously by Seelig⁴² and Suomalainen.30

The folding-coupled binding mechanism that has been proposed for several peptides⁵⁵ has also been reported for piscidins. 15 Partitioning coefficients previously determined for amphipathic peptides Ac-18A-NH₂⁵⁶ and melittin⁵⁷ to PC liposomes indicate interaction energies of -7.9 and -7.6 kcal/ mol, which correspond to $\log K_{\rm lip}$ values of 5.7 and 5.5. The higher partitioning coefficient for P1 to lipid monolayers reported here can be partially accounted by P1's stronger amphipathicity compared to Ac-18A-NH₂.⁵⁸ However, there might be a principal difference in partition coefficients measured in liposomes and monolayers.^{27,55} Although the partitioning coefficients obtained from our monolayer experiments are calculated at the monolayer-bilayer equivalence pressure, this binding equilibrium may not be identical to the binding equilibrium in bilayer liposomes. Currently, there are no liposome partitioning data for P1 reported and therefore a systematic side-by-side comparison of P1 insertion in liposomes and monolayers of the same composition would be a timely task. The nearly perfect amphipathicity of P1 and P3 helices and their complementary interactions with surrounding phospholipids 16-18 raise the question of how much these interactions stabilize the helix. Because we have no means to prevent helix formation on the surface of phospholipid membranes while measuring affinity, we cannot independently estimate the energies of the two coupled processes, binding and folding. These two experimentally inseparable energies, however, can be addressed in MD simulations.

In an ideal situation when a hydrophobic substance intercalates into an expanded lipid monolayer, its partition coefficient $(K_{\rm lip})$ would reflect the hydrophobic energy component of exclusion from the aqueous phase to the surface plus the energy of favorable interactions with lipids. Together, they would constitute the negative chemical free energy of intercalation, $\Delta G_{\rm chem}$. Compression of the monolayer increases the lateral pressure p, which counteracts the insertion by adding a positive mechanical energy component, $\Delta G_{\rm mech} = p \cdot A_{\rm S}$, where $A_{\rm S}$ is the cross-sectional area of the guest molecule. If pressure is distributed uniformly across the monolayer and the guest can be either inserted or unbound, then the equilibrium can be written in a simple form 30

$$-RT \ln(K_{\text{lip}}) = \Delta G_{\text{chem}} + p \cdot A_{S}$$
(3)

with ΔG_{chem} negative and $p \cdot A_S$ positive, this equation identifies a critical pressure at which the chemical and mechanical terms cancel each other, defining it as the equipartitioning point. This critical pressure can be either below or above the

monolayer—bilayer equivalence pressure $p_{\rm B}$. A series of measurements of $K_{\rm lip}$ at different surface pressures would provide values for both $A_{\rm S}$ and $\Delta G_{\rm chem}$. For permeation, an important characteristic of the guest molecule is whether it remains in the monolayer when pressure reaches $p_{\rm B}$. If the sum of $\Delta G_{\rm chem}$ and $p_{\rm B}$ - $A_{\rm S}$ is substantial and negative, the substance will have sufficient affinity to insert itself in a bilayer packed to the same density as a monolayer at $p_{\rm B}$ and a small $A_{\rm S}$ value will result in increased intercalation. In contrast, low chemical affinity or large $A_{\rm S}$ values may become prohibitive for the intercalation of the substance and permeation across the membrane.

The data presented above, however, depict more complex pictures of piscidin intercalation into phospholipid and LPS monolayers. Both systems, especially LPS, are highly stratified and there is apparently more than one bound state for the peptide. It is also possible that some compacting transitions represent reorientation rather than complete expulsion from a deeply bound state. The analysis of different contributions into P1 affinities toward phospholipid and LPS monolayers is illustrated in Figure 9. The partition coefficients $K_{\rm lip}$ in Table 1

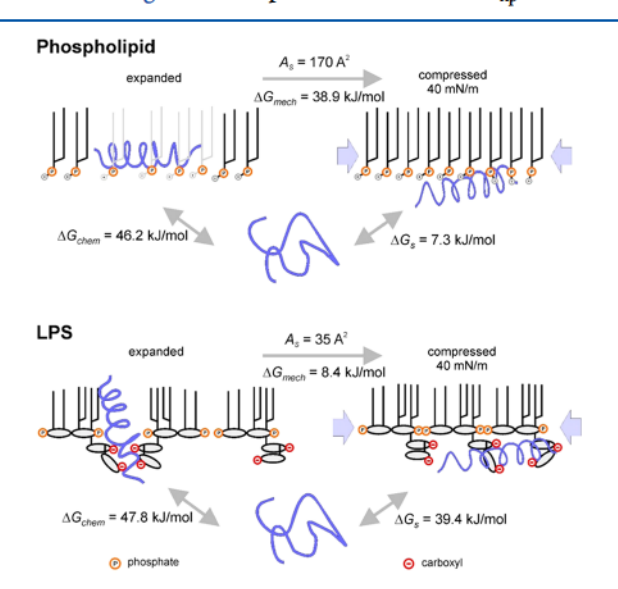


Figure 9. Insertion models proposed to describe the thermodynamics of P1 interacting with the phospholipid and LPS monolayers. The free energies of the peptide binding to relaxed films $\Delta G_{\rm chem}$ minus the contribution of lateral pressure predict a much higher P1 affinity to fully compressed LPS monolayers compared to phospholipid monolayers. The values for $\Delta G_{\rm s}$ are estimated from two other ΔG parameters in the thermodynamic cycle.

are converted into the free energies of binding to expanded films when binding is unopposed by lateral pressure. The work of elevated lateral pressure ($p=40~{\rm mN/m}$) driving the compaction/expulsion transition is calculated as $p \cdot A_{\rm S}$. The completion of each thermodynamic cycle predicts the affinity of P1 toward compressed films. P1 binding to phospholipids with $A_{\rm S}=170~{\rm \AA}^2$ mounts a strong opposition that almost completely negates the chemical component of the binding energy. In contrast, a small P1's footprint among LPS molecules allows for continuous presence inside the LPS layer as the affinity remains high over the entire pressure interval. In contrast to phospholipids, which have a \sim 5 Å layer of oxygen-carrying groups capable of interacting with positive sidechains of piscidins, LPS presents a 20 Å thick layer of

negative charges carried by phosphates on glucosamine and carboxyls on 2-keto-3-deoxyoctonate (KDO) sugar moieties, ³³ which would allow for retention of positively charged peptides at the surface in a variety of different conformations at any pressure.

Langmuir experiments combined with interfacial potential recording (Figure 2) have also indicated that despite four negative charges carried by LPS molecules (partially neutralized by divalent ions), the measured interfacial potential is decisively positive (+250 mV). This indicates a strong inwardly directed dipole, similar to that described for phospholipids, 44 which is likely generated by ordered solvating water. 45,59 This dipole potential, positive inside the outer membrane, will be an additional impediment for permeation of cationic drugs.

We should note that P3 exhibits an $A_{\rm S}$ at the air—water and LPS interfaces that is twice as large as P1 (Table 1), suggesting that it may form dimers. Indeed, P3 is structurally different from P1 in the sense that it has three GXXXG and GXXXXG motifs (i.e., G8 \rightarrow G13, G13 \rightarrow G17, and G17 \rightarrow G22) supporting coiling 60 whereas P1 has only one (i.e., G8 \rightarrow G13). The question remains whether P3 dimerizes in solution or requires a water interface, membrane surface, or DNA scaffolding 47 for interaction. The glycines also increase flexibility of the α -helix, which may adversely affect the membrane-breaking capacity.

The cross-sectional areas of 30-35 Å² estimated for P1 on the bare air-water interface and in LPS layers are smaller than the footprint of an "upright" helix oriented normally to the interface. The spatial distribution of negative charges in the LPS layer is not as planar as the distribution of phosphates in a regular phospholipid layer. In the LPS environment, piscidin α helices may be randomly oriented or unfolded. The Langmuir data support the inference that the piscidin's affinity and small footprint are sufficient to drive intercalation into the outer LPS layer of the native bacterial envelope. Indeed, a substantial amount of the guest molecule remaining in the monolayer at pressures that are above the monolayer-bilayer equivalence pressure directly reflects the thermodynamic capacity of the substance to intercalate into the outer membrane. The 22amino-acid chain with a free amino terminus, two Arg, one Lys, and four His residues potentially carries 8 positive charges under permissive conditions. It may therefore form multiple contacts with carboxyls and phosphates, replacing divalent ions and possibly separating LPS molecules, thus creating structural defects. These defects would further assist peptide permeation through the outer layer. We may refer to this mechanism as "self-promoted uptake" of a positively charged peptide that tends to displace the divalent cations that tightly link LPS molecules.3 Not coincidentally, the loss of a special kinase that phosphorylates LPS makes E. coli less susceptible to the highly cationic human defense peptide cathelicidin.61 Similarly, commensal bacteria from the phylum Bacteroides and four other phyla must remove a phosphate group from their LPS using LpxF phosphatase to survive high concentrations of AMPs during intestinal inflammation. 62 Future studies would require experiments with more "natural" bacterial LPS because having longer polysaccharide chains may influence piscidin accumulation and permeability. Additionally, the possibility of uncoiled piscidin penetration through porins should be addressed as well. Upon wedging between LPS molecules and penetrating into the periplasm, piscidins meet layers of phospholipids where they may form amphipathic helices and attack the energized cytoplasmic membrane.

Our estimation of P1's interaction area (~170 Å2) with phospholipids is highly consistent with NMR data and MD simulations, predicting a footprint of 190–220 $\mbox{Å}^{2.16,18,20}$ For piscidins forming well-organized amphipathic helices laying almost flat on the surface of the phospholipid bilayer, the crosssectional interaction area is maximal. 18 For this reason, the helix is firmly anchored and stabilized on the surface. When the helix is driven into the membrane by high electric field, it does not simply permeate but rather breaks the bilayer to form transient pores or leakage-competent defects. 17,19 Our data do not support alamethicin-like barrel-stave channels^{63,64} as structural defects formed by piscidins, but rather toroidal lipid pores that form and expand in MD simulations under an elevated voltage of 0.2 V across the membrane. 19 Formation of such pores or surface defects 17,19 with a peptide-stabilized rim likely results from thinning of the bilayer and curvature generation by the peptide. Our direct patch-clamp recordings of P1- and P3-formed pores in the inner membrane of E. coli (Figure 6) provide ultimate proof to the pivotal concept that the primary target for piscidins is the lipid bilayer of the bacterial cytoplasmic membrane. The formation of conductive structures is indeed steeply voltage dependent and is seen at voltages below 100 mV, implying that not even fully energized bacteria⁵¹ will also be susceptible to piscidins. The preferential activity of vertebrate piscidins against bacteria and not against an organism's own tissues is due to the fact that the membrane-perforating capacity is greatly enhanced by the high membrane potential, which is typically present across the membranes of bacteria. Highly energized mitochondrial membranes are hidden deep inside vertebrate cells and not directly exposed to piscidins.

Our previous data²⁰ illustrated that piscidins, when added from the cytoplasmic side, also exert a stimulating effect on bacterial mechanosensitive channels MscS and MscL by shifting their activation curves to the left and thus assisting activation by tension. This predisposition of MS channels to opening could be a part of the bacteriostatic mechanism of piscidins. In this work, we have shown that P1 presented to the periplasmic side of the inner membrane produces a very small effect on MS channels. The sidedness of P1's effect is likely due to the asymmetric structure of these channels and more cytoplasmic positions of their gates.⁶⁵ Further growth experiments have shown that the $\Delta mscS$, $\Delta mscK$, and $\Delta mscL$ E. coli strain deprived of three major MS channels does not show any advantage over WT in surviving piscidins, indicating that mechanosensitive channels may not be primary targets for growth inhibition by piscidins.

CONCLUSIONS

The data presented above show that piscidins 1 and 3 avidly intercalate into both phospholipid and LPS monolayers but have a higher overall affinity for LPS. The monolayer system with controlled area per molecule allowed us to monitor the partitioning of peptides at different lateral pressures and extract the intercalation area taken by a single peptide in the plane of the monolayer. The area of P1 was 5-fold larger when bound to phospholipids compared to LPS, indicating that it has different modes of interaction with the two interfaces. The larger area of P1 is consistent with its α -helical conformation bound parallel to the phospholipid monolayer plane, whereas the more compact state of P1 on LPS may suggest either an upright α -

helix or disordered chain conformation. Direct patch-clamp recordings performed on the inner membrane of E. coli have shown that both piscidins form fluctuating conductive pores at elevated membrane potentials that are normally present in energized bacteria. We conclude that the specificity against Gram-negative bacteria begins with preferential accumulation of peptides in the outer LPS layer of the bacterial envelope, followed by penetration into the periplasm as ordered or disordered chains. In the periplasm, piscidins form amphipathic α -helices on contact with phospholipids and gain the capacity to attack the energy-coupling inner membrane.

AUTHOR INFORMATION

Corresponding Author

Sergei Sukharev — Biology Department, University of Maryland—College Park, College Park, Maryland 20742, United States; orcid.org/0000-0002-4807-9665; Phone: 301-405-6923; Email: sukharev@umd.edu

Authors

- Hannah Cetuk Biology Department, University of Maryland—College Park, College Park, Maryland 20742, United States
- Joseph Maramba Biology Department, University of Maryland—College Park, College Park, Maryland 20742, United States
- Madolyn Britt Biology Department, University of Maryland College Park, College Park, Maryland 20742, United States
- Alison J. Scott Department of Microbial Pathogenesis, University of Maryland—Baltimore, Baltimore, Maryland 21201, United States
- Robert K. Ernst Department of Microbial Pathogenesis, University of Maryland—Baltimore, Baltimore, Maryland 21201, United States
- Mihaela Mihailescu Institute for Bioscience and Biotechnology Research, Rockville, Maryland 20850, United States
- Myriam L. Cotten Department of Applied Science, College of William and Mary, Williamsburg, Virginia 23185, United States; Occid.org/0000-0002-6732-1736

Complete contact information is available at: https://pubs.acs.org/10.1021/acs.langmuir.0c00017

Notes

The authors declare no competing financial interest.

ACKNOWLEDGMENTS

The authors thank Dr. Andriy Anishkin for critical suggestions. The work was partially supported by NIH R01AI135015 to S.S. and by the National Science Foundation (MCB-1716608 to M.L.C. and MCB-1714164 to M.M.).

REFERENCES

- (1) Teixeira, V.; Feio, M. J.; Bastos, M. Role of lipids in the interaction of antimicrobial peptides with membranes. *Prog. Lipid Res.* **2012**, *51*, 149–177.
- (2) Last, N. B.; Schlamadinger, D. E.; Miranker, A. D. A common landscape for membrane-active peptides. *Protein Sci.* 2013, 22, 870–882.
- (3) Hancock, R. E. Peptide antibiotics. Lancet 1997, 349, 418-422.
- (4) Chen, W. F.; Huang, S. Y.; Liao, C. Y.; Sung, C. S.; Chen, J. Y.; Wen, Z. H. The use of the antimicrobial peptide piscidin (PCD)-1 as a novel anti-nociceptive agent. *Biomaterials* 2015, 53, 1–11.
- (5) Masso-Silva, J. A.; Diamond, G. Antimicrobial peptides from fish. *Pharmaceuticals* 2014, 7, 265–310.

- (6) Milne, D. J.; Fernandez-Montero, A.; Gundappa, M. K.; Wang, T.; Acosta, F.; Torrecillas, S.; Montero, D.; Zou, J.; Sweetman, J.; Secombes, C. J. An insight into piscidins: The discovery, modulation and bioactivity of greater amberjack, *Seriola dumerili*, piscidin. *Mol. Immunol.* 2019, 114, 378–388.
- (7) Silphaduang, U.; Noga, E. J. Peptide antibiotics in mast cells of fish. *Nature* 2001, 414, 268–269.
- (8) Lauth, X.; Shike, H.; Burns, J. C.; Westerman, M. E.; Ostland, V. E.; Carlberg, J. M.; Van Olst, J. C.; Nizet, V.; Taylor, S. W.; Shimizu, C.; Bulet, P. Discovery and characterization of two isoforms of moronecidin, a novel antimicrobial peptide from hybrid striped bass. *J. Biol. Chem.* 2002, 277, 5030–5039.
- (9) Chekmenev, E. Y.; Vollmar, B. S.; Forseth, K. T.; Manion, M. N.; Jones, S. M.; Wagner, T. J.; Endicott, R. M.; Kyriss, B. P.; Homem, L. M.; Pate, M.; He, J.; Raines, J.; Gor'kov, P. L.; Brey, W. W.; Mitchell, D. J.; Auman, A. J.; Ellard-Ivey, M. J.; Blazyk, J.; Cotten, M. Investigating molecular recognition and biological function at interfaces using piscidins, antimicrobial peptides from fish. *Biochim. Biophys. Acta, Biomembr.* 2006, 1758, 1359—1372.
- (10) Lee, S. A.; Kim, Y. K.; Lim, S. S.; Zhu, W. L.; Ko, H.; Shin, S. Y.; Hahm, K. S.; Kim, Y. Solution structure and cell selectivity of piscidin 1 and its analogues. *Biochemistry* 2007, 46, 3653–3663.
- (11) Wang, G. Database-Guided Discovery of Potent Peptides to Combat HIV-1 or Superbugs. *Pharmaceuticals* 2013, 6, 728-758.
- (12) Hu, H.; Guo, N.; Chen, S.; Guo, X.; Liu, X.; Ye, S.; Chai, Q.; Wang, Y.; Liu, B.; He, Q. Antiviral activity of Piscidin 1 against pseudorabies virus both in vitro and in vivo. *Virol. J.* 2019, 16, No. 95.
- (13) Lin, H. J.; Huang, T. C.; Muthusamy, S.; Lee, J. F.; Duann, Y. F.; Lin, C. H. Piscidin-1, an antimicrobial peptide from fish (hybrid striped bass *Morone saxatilis* x *M. chrysops*), induces apoptotic and necrotic activity in HT1080 cells. *Zool. Sci.* 2012, 29, 327–332.
- (14) Sung, W. S.; Lee, J.; Lee, D. G. Fungicidal effect of piscidin on *Candida albicans*: pore formation in lipid vesicles and activity in fungal membranes. *Biol. Pharm. Bull.* 2008, 31, 1906–1910.
- (15) Campagna, S.; Saint, N.; Molle, G.; Aumelas, A. Structure and mechanism of action of the antimicrobial peptide piscidin. *Biochemistry* 2007, 46, 1771–1778.
- (16) Perrin, B. S., Jr.; Tian, Y.; Fu, R.; Grant, C. V.; Chekmenev, E. Y.; Wieczorek, W. E.; Dao, A. E.; Hayden, R. M.; Burzynski, C. M.; Venable, R. M.; Sharma, M.; Opella, S. J.; Pastor, R. W.; Cotten, M. L. High-resolution structures and orientations of antimicrobial peptides piscidin 1 and piscidin 3 in fluid bilayers reveal tilting, kinking, and bilayer immersion. *J. Am. Chem. Soc.* 2014, 136, 3491–3504.
- (17) Mihailescu, M.; Sorci, M.; Seckute, J.; Silin, V. I.; Hammer, J.; Perrin, B. S., Jr.; Hernandez, J. I.; Smajic, N.; Shrestha, A.; Bogardus, K. A.; Greenwood, A. I.; Fu, R.; Blazyk, J.; Pastor, R. W.; Nicholson, L. K.; Belfort, G.; Cotten, M. L. Structure and Function in Antimicrobial Piscidins: Histidine Position, Directionality of Membrane Insertion, and pH-Dependent Permeabilization. *J. Am. Chem. Soc.* 2019, 141, 9837–9853.
- (18) Perrin, B. S., Jr.; Sodt, A. J.; Cotten, M. L.; Pastor, R. W. The Curvature Induction of Surface-Bound Antimicrobial Peptides Piscidin 1 and Piscidin 3 Varies with Lipid Chain Length. *J. Membr. Biol.* 2015, 248, 455–467.
- (19) Perrin, B. S., Jr.; Fu, R.; Cotten, M. L.; Pastor, R. W. Simulations of Membrane-Disrupting Peptides II: AMP Piscidin 1 Favors Surface Defects over Pores. *Biophys. J.* 2016, 111, 1258–1266.
- (20) Comert, F.; Greenwood, A.; Maramba, J.; Acevedo, R.; Lucas, L.; Kulasinghe, T.; Cairns, L. S.; Wen, Y.; Fu, R.; Hammer, J.; Blazyk, J.; Sukharev, S.; Cotten, M. L.; Mihailescu, M. The host-defense peptide piscidin P1 reorganizes lipid domains in membranes and decreases activation energies in mechanosensitive ion channels. *J. Biol. Chem.* 2019, 294, 18557–18570.
- (21) Hayden, R. M.; Goldberg, G. K.; Ferguson, B. M.; Schoeneck, M. W.; Libardo, M. D.; Mayeux, S. E.; Shrestha, A.; Bogardus, K. A.; Hammer, J.; Pryshchep, S.; Lehman, H. K.; McCormick, M. L.; Blazyk, J.; Angeles-Boza, A. M.; Fu, R.; Cotten, M. L. Complementary Effects of Host Defense Peptides Piscidin 1 and Piscidin 3 on DNA

- and Lipid Membranes: Biophysical Insights into Contrasting Biological Activities. J. Phys. Chem. B 2015, 119, 15235-15246.
- (22) Epand, R. M.; Épand, R. F. Lipid domains in bacterial membranes and the action of antimicrobial agents. *Biochim. Biophys. Acta, Biomembr.* 2009, 1788, 289–294.
- (23) Fjell, C. D.; Hiss, J. A.; Hancock, R. E.; Schneider, G. Designing antimicrobial peptides: form follows function. *Nat. Rev. Drug Discovery* 2012, 11, 37–51.
- (24) Épand, R. M.; Walker, C.; Epand, R. F.; Magarvey, N. A. Molecular mechanisms of membrane targeting antibiotics. *Biochim. Biophys. Acta, Biomembr.* 2016, 1858, 980–987.
- (25) Hancock, R. E. The bacterial outer membrane as a drug barrier. *Trends Microbiol.* 1997, 5, 37–42.
- (26) Delcour, A. H. Outer membrane permeability and antibiotic resistance. *Biochim. Biophys. Acta, Proteins Proteomics* 2009, 1794, 808-816.
- (27) Seelig, A. The use of monolayers for simple and quantitative analysis of lipid-drug interactions exemplified with dibucaine and substance P. Cell Biol. Int. Rep. 1990, 14, 369–380.
- (28) Brockman, H. Lipid monolayers: why use half a membrane to characterize protein-membrane interactions? *Curr. Opin. Struct. Biol.* 1999, 9, 438–443.
- (29) Seelig, A. Local anesthetics and pressure: a comparison of dibucaine binding to lipid monolayers and bilayers. *Biochim. Biophys. Acta, Biomembr.* 1987, 899, 196–204.
- (30) Suomalainen, P.; Johans, C.; Soderlund, T.; Kinnunen, P. K. Surface activity profiling of drugs applied to the prediction of bloodbrain barrier permeability. *J. Med. Chem.* 2004, 47, 1783–1788.
- (31) Rowe, I.; Guo, M.; Yasmann, A.; Cember, A.; Sintim, H. O.; Sukharev, S. Membrane Affinity of Platensimycin and Its Dialkylamine Analogs. *Int. J. Mol. Sci.* 2015, *16*, 17909–17932.
- (32) Chekmenev, E. Y.; Jones, S. M.; Nikolayeva, Y. N.; Vollmar, B. S.; Wagner, T. J.; Gor'kov, P. L.; Brey, W. W.; Manion, M. N.; Daugherty, K. C.; Cotten, M. High-field NMR studies of molecular recognition and structure-function relationships in antimicrobial piscidins at the water-lipid bilayer interface. J. Am. Chem. Soc. 2006, 128, 5308–5309.
- (33) Qureshi, N.; Takayama, K.; Mascagni, P.; Honovich, J.; Wong, R.; Cotter, R. J. Complete structural determination of lipopolysaccharide obtained from deep rough mutant of *Escherichia coli*. Purification by high performance liquid chromatography and direct analysis by plasma desorption mass spectrometry. *J. Biol. Chem.* 1988, 263, 11971–11976.
- (34) Galanos, C.; Luderitz, O.; Westphal, O. A new method for the extraction of R lipopolysaccharides. *Eur. J. Biochem.* 1969, 9, 245–249.
- (35) Levina, N.; Tötemeyer, S.; Stokes, N. R.; Louis, P.; Jones, M. A.; Booth, I. R. Protection of *Escherichia coli* cells against extreme turgor by activation of MscS and MscL mechanosensitive channels: identification of genes required for MscS activity. *EMBO J.* 1999, 18, 1730–1737.
- (36) Kamaraju, K.; Smith, J.; Wang, J.; Roy, V.; Sintim, H. O.; Bentley, W. E.; Sukharev, S. Effects on membrane lateral pressure suggest permeation mechanisms for bacterial quorum signaling molecules. *Biochemistry* 2011, *50*, 6983–6993.
- (37) Kamaraju, K.; Sukharev, S. The membrane lateral pressureperturbing capacity of parabens and their effects on the mechanosensitive channel directly correlate with hydrophobicity. *Biochemistry* 2008, 47, 10540–10550.
- (38) Edwards, M. D.; Black, S.; Rasmussen, T.; Rasmussen, A.; Stokes, N. R.; Stephen, T. L.; Miller, S.; Booth, I. R. Characterization of three novel mechanosensitive channel activities in *Escherichia coli*. *Channels* 2012, 6, 272–281.
- (39) Martinac, B.; Buechner, M.; Delcour, A. H.; Adler, J.; Kung, C. Pressure-sensitive ion channel in *Escherichia coli. Proc. Natl. Acad. Sci. U.S.A.* 1987, 84, 2297–2301.
- (40) Akitake, B.; Anishkin, A.; Sukharev, S. The "dashpot" mechanism of stretch-dependent gating in MscS. J. Gen. Physiol. 2005, 125, 143–154.

- (41) Begot, C.; Desiner, I.; Daudin, J. D.; Labadie, J. C.; Lebert, A. Recommendations for calculating growth parameters by optical density measurements. *J. Microbiol. Methods* 1996, 25, 225–232.
- (42) Seelig, A.; Gottschlich, R.; Devant, R. M. A method to determine the ability of drugs to diffuse through the blood-brain barrier. *Proc. Natl. Acad. Sci. U.S.A.* 1994, 91, 68–72.
- (43) Gerebtzoff, G.; Li-Blatter, X.; Fischer, H.; Frentzel, A.; Seelig, A. Halogenation of drugs enhances membrane binding and permeation. *ChemBioChem* 2004, 5, 676–684.
- (44) Brockman, H. Dipole potential of lipid membranes. *Chem. Phys. Lipids* 1994, 73, 57–79.
- (45) Zhou, F.; Schulten, K. Molecular-Dynamics Study of a Membrane Water Interface. J. Phys. Chem. A. 1995, 99, 2194-2207.
- (46) Dahim, M.; Mizuno, N. K.; Li, X. M.; Momsen, W. E.; Momsen, M. M.; Brockman, H. L. Physical and photophysical characterization of a BODIPY phosphatidylcholine as a membrane probe. *Biophys. J.* 2002, *83*, 1511–1524.
- (47) Libardo, M. D. J.; Bahar, A. A.; Ma, B.; Fu, R.; McCormick, L. E.; Zhao, J.; McCallum, S. A.; Nussinov, R.; Ren, D.; Angeles-Boza, A. M.; Cotten, M. L. Nuclease activity gives an edge to host-defense peptide piscidin 3 over piscidin 1, rendering it more effective against persisters and biofilms. *FEBS J.* 2017, 284, 3662–3683.
- (48) Kim, J. K.; Lee, S. A.; Shin, S.; Lee, J. Y.; Jeong, K. W.; Nan, Y. H.; Park, Y. S.; Shin, S. Y.; Kim, Y. Structural flexibility and the positive charges are the key factors in bacterial cell selectivity and membrane penetration of peptoid-substituted analog of Piscidin 1. *Biochim. Biophys. Acta, Biomembr.* 2010, 1798, 1913–1925.
- (49) Jiang, Z.; Vasil, A. I.; Vasil, M. L.; Hodges, R. S. "Specificity Determinants" Improve Therapeutic Indices of Two Antimicrobial Peptides Piscidin 1 and Dermaseptin S4 Against the Gram-negative Pathogens Acinetobacter baumannii and Pseudomonas aeruginosa. Pharmaceuticals 2014, 7, 366–391.
- (50) Skulachev, V. P. Chemiosmotic systems in bioenergetics: H(+)-cycles and Na(+)-cycles. *Biosci. Rep.* 1991, 11, 387–441. discussion 441–444
- (51) Bot, C. T.; Prodan, C. Quantifying the membrane potential during *E. coli* growth stages. *Biophys. Chem.* 2010, 146, 133–137.
- (52) Kamaraju, K.; Gottlieb, P. A.; Sachs, F.; Sukharev, S. Effects of GsMTx4 on bacterial mechanosensitive channels in inside-out patches from giant spheroplasts. *Biophys. J.* 2010, *99*, 2870–2878.
- (53) Seydel, U.; Koch, M. H.; Brandenburg, K. Structural polymorphisms of rough mutant lipopolysaccharides Rd to Ra from Salmonella minnesota. J. Struct. Biol. 1993, 110, 232–243.
- (54) Redeker, C.; Briscoe, W. H. Interactions between Mutant Bacterial Lipopolysaccharide (LPS-Ra) Surface Layers: Surface Vesicles, Membrane Fusion, and Effect of Ca(2+)and Temperature. *Langmuir* 2019, 35, 15739–15750.
- (55) White, S. H.; Wimley, W. C. Membrane protein folding and stability: physical principles. *Annu. Rev. Biophys. Biomol. Struct.* 1999, 28, 319–365.
- (56) Gazzara, J. A.; Phillips, M. C.; Lund-Katz, S.; Palgunachari, M. N.; Segrest, J. P.; Anantharamaiah, G. M.; Rodrigueza, W. V.; Snow, J. W. Effect of vesicle size on their interaction with class A amphipathic helical peptides. *J. Lipid Res.* 1997, 38, 2147–2154.
- (57) Ladokhin, A. S.; White, S. H. Folding of amphipathic alphahelices on membranes: energetics of helix formation by melittin. *J. Mol. Biol.* 1999, 285, 1363–1369.
- (58) Hristova, K.; Wimley, W. C.; Mishra, V. K.; Anantharamiah, G. M.; Segrest, J. P.; White, S. H. An amphipathic alpha-helix at a membrane interface: a structural study using a novel X-ray diffraction method. *J. Mol. Biol.* 1999, 290, 99–117.
- (59) Gawrisch, K.; Ruston, D.; Zimmerberg, J.; Parsegian, V. A.; Rand, R. P.; Fuller, N. Membrane dipole potentials, hydration forces, and the ordering of water at membrane surfaces. *Biophys. J.* 1992, 61, 1213–1223.
- (60) Popot, J. L.; Engelman, D. M. Helical membrane protein folding, stability, and evolution. *Annu. Rev. Biochem.* **2000**, *69*, 881–922.

- (61) Bociek, K.; Ferluga, S.; Mardirossian, M.; Benincasa, M.; Tossi, A.; Gennaro, R.; Scocchi, M. Lipopolysaccharide Phosphorylation by the WaaY Kinase Affects the Susceptibility of *Escherichia coli* to the Human Antimicrobial Peptide LL-37. *J. Biol. Chem.* 2015, 290, 19933–19941.
- (62) Cullen, T. W.; Schofield, W. B.; Barry, N. A.; Putnam, E. E.; Rundell, E. A.; Trent, M. S.; Degnan, P. H.; Booth, C. J.; Yu, H.; Goodman, A. L. Gut microbiota. Antimicrobial peptide resistance mediates resilience of prominent gut commensals during inflammation. *Science* 2015, 347, 170–175.
- (63) Wimley, W. C. Describing the mechanism of antimicrobial peptide action with the interfacial activity model. ACS Chem. Biol. 2010, 5, 905–917.
- (64) Rahaman, A.; Lazaridis, T. A thermodynamic approach to alamethicin pore formation. *Biochim. Biophys. Acta, Biomembr.* 2014, 1838, 98–105.
- (65) Strop, P.; Bass, R.; Rees, D. C. Prokaryotic mechanosensitive channels. Adv. Protein Chem. 2003, 63, 177-209.